Aluminum Distribution in Low Si/Al Zeolites: Dehydrated Na−Clinoptilolite

A. Rabdel Ruiz-Salvador,*,† Dewi W. Lewis,‡ Jesús Rubayo-Soneira,§ Gerardo Rodríguez-Fuentes,† L. Rene Sierra,|| and C. Richard A. Catlow⊥

Department of Materials Science, Zeolites Engineering Lab., IMRE-Fac. Physics, University of Havana, Havana 10400, Cuba, Department of Materials Science and Metallurgy, University of Cambridge, Pembroke Street, Cambridge CB2 3QZ, U.K., Department Physics, Fac. Sciences, Higher Pedagogical Inst. EJV, Ciudad Libertad, Playa, Havana 19220, Cuba, Inst. Superior Ciencias y Tecnología Nucleares, Ave. Salvador Allende y Luaces, Havana 10600, Cuba, and Davy Faraday Research Laboratory, Royal Institution of Great Britain, 21 Albemarle Street, London W1X 4BS, U.K.

Received: May 12, 1998; In Final Form: July 28, 1998

We have investigated the siting and distribution of Al atoms in the zeolite clinoptilolite using periodic lattice simulation techniques. A novel procedure is presented for the study of the unresolved problem concerning the Al atoms siting in heulandite-structured materials. The resulting structural models are in excellent agreement with experimental studies and show preferential aluminum siting at T2 and minimal aluminum occupancy of T5. We show how Al−Al and Al−Na interactions are important in the siting of Al atoms in low Si/Al regimes. We also show the importance of lattice relaxation in finding the lowest energy aluminum distribution and the failure of standard Monte Carlo techniques in this context.

1. Introduction

The framework aluminosilicates, typified by zeolites, have physical properties which are widely exploited on an industrial scale. In particular, their ion exchange capacity is currently utilized in the detergent and nuclear industries for the removal of metal cations from solution: softening water in the case of detergency and removal of radioactive species from contaminated solutions in the nuclear industry. The property of ion exchange is imparted to these materials by the ability of loosely bound extraframework cations, present in the cages and channels, to be replaced by other cations. The inclusion of these extraframework cations requires the presence of aluminum (or other low valent metal ions) in the framework, thereby producing an effective negative charge on the framework, which is charge compensated by the presence of the extraframework cations. Thus, the concentration of exchangeable cations decreases with the Si/Al ratio. The position of these extraframework cations can, in some cases, be identified by diffraction methods. However, the precise siting and distribution of the aliovalent ions in the tetrahedral framework sites, which can have a profound effect on the physical properties of the materials, remains one of the most intriguing and difficult problems concerning the structural physics and chemistry of these solids and has been the subject of many experimental[1−4] and theoretical studies.[5−8]

Both ^{29}Si and ^{27}Al NMR[9,10] can provide information on the local distribution of Si and Al, giving information on the immediate environment of a particular tetrahedral site. However, determination of the spatial distribution of Al in the whole cell is difficult by experimental methods, because from diffraction methods it is difficult to distinguish between Si and Al atoms in tetrahedral sites. Theoretical studies, using both quantum chemical calculations[5,6] and simulation methods,[7,8] have focused on local structural analysis rather than Al distribution.

Quantum chemical studies of such microporous structures have a strong dependence on the input crystallographic data, because these complex structures are typically treated using a cluster approach[5,6] in which properties are determined for a finite fragment, and long-range effects are ignored. However, we note that periodic quantum mechanical (QM) calculations are now feasible.[11,12] A consequence of the use of clusters is that the calculations consider only short-range interactions. For example Derouane and Fripiat found for ZSM-5[6] that Al atoms preferably occupy T2 sites which exhibit the largest T−O distances, as in the experimental data used to construct the clusters.[13] More recent experimental structure determinations resulted in almost equal T−O distance for all T sites,[14] and further calculations based on this structure did not find any significant difference between the Al occupancy in the different T sites.[15]

Simulation methods[16] using periodic boundary conditions include long-range interactions, and thus the cluster size limitation is eliminated. Most studies of Si−Al ordering were performed employing the Mott−Littleton methodology,[17] introducing Al atoms as "defects" in an all-silica framework. Atomistic structures obtained by this technique reproduce very well the local environment around the defects. The calculated defect energies are used as a measure of the feasibility of incorporating Al atoms at the framework site, allowing any preferential Al sites to be identified.

It was demonstrated that aliovalent substitution in tetrahedral sites is accompanied by distortion[18−20] of the first and even the second coordination sphere of the substituted T atom. Both the stresses induced by such distortions and the electrostatic interactions between the Al substitutionals are factors influencing Lowenstein's[21] and Dempsey's rules.[22] Lowenstein's rule states

* Corresponding author. E-mail: rabdel@imre.fmq.uh.edu.cu.
† University of Havana.
‡ University of Cambridge.
§ Higher Pedagogical Institute.
|| Inst. Superior Ciencias y Tecnología Nucleares.
⊥ Royal Institution of Great Britain.

10.1021/jp982211k CCC: $15.00
Published on Web 09/26/1998

that Al−O−Al bridges are forbidden, and is generally observed; although there is some evidence for non-Lowensteinian distribution in high-temperature synthesized sodalite materials.[23] Indeed, the energetic basis of Lowenstein's rule was investigated[24] using the simulations techniques discussed above (and used in this paper). Bell et al.[24] studied three different aluminum distributions and three different sodium distributions in zeolite A and found a weak thermodynamic preference for a Lowensteinian model. According to Dempsey's rule, Al atoms substitute so that they are distributed as widely as possible for a given Si/Al (i.e., Al−Al distances are maximized), and it was shown that in some cases the rule is fulfilled.[25] However, some authors found cases in which Al−O−Si−O−Al linkages were stable as they helped to bind divalent extraframework cations.[26] We should also note that recent QM studies of small aluminosilicate species, considered to be important precursors to the framework structure, suggested that Lowensteinian behavior is a function of the energetics of such small species,[27] and that it is the energetics of the formation of Al−O−Al bridges in solution that is responsible for Lowenstein's rule.

In considering the location of Al atoms in zeolites, we note two limiting cases. In high-silica zeolites the Al ions can be considered as dilute impurities in a siliceous matrix, and the framework will relax only locally without major distortions to the structure. Thus, we can consider that the Al are distributed homogeneously. On the other hand, when the Si/Al ratio is equal to one a strict alternation of Si and Al is expected, such as in the case of zeolite A.[28] However, the problem becomes very complicated when one considers zeolites having Si/Al ratios between the above two limiting cases; a prime example is the zeolite clinoptilolite with a Si/Al ratio of ∼5.

Clinoptilolite is the most common naturally occurring zeolite and is isostructural with heulandite. It belongs to the seventh Breck classification group,[29] characterized by 4−4−1 secondary building units forming a 2-dimensional channel systems (Figure 1). This material has a strong affinity for heavy metal ions,[30] a property that is exploited for environmental pollution control including radioactive waste decontamination.[31]

Despite the wide use of clinoptilolite in industry, theoretical studies on this zeolite are scarce.[32−34] Slaughter et al. investigated the bonding through calculations of partial binding energies,[32] whereas Channon et al. carried out computer simulation studies on the loading and location of water molecules.[33] Channon et al.,[34] more recently, identified that consideration of extraframework cations and long-range effects are critical in obtaining good agreement with experimentally determined Al site occupations. Indeed, they identified a number of unit cell configurations which correlate well with experiment. However, only a limited number of generated configurations were optimized and there remains the question of whether there are alternative stable configurations. Nevertheless, these studies and our recent work on internal T−O bending vibration frequency of some metal−clinoptilolite forms[35] suggest that such simulation techniques are wholly suitable for the study of the structural properties of this class of zeolite.

In the present paper we propose a novel procedure to investigate the energetics of Al distribution over the tetrahedral sites in the clinoptilolite structure (although the method can be generally applied to low Si/Al materials). In the next section we present the methodological aspects of our approach including details of the interatomic potentials and minimization procedures employed. We calculate the lattice energies of different configurations and we compare our results with those obtained from experimental structural refinements. We then discuss our results emphasizing the role of interaction between Al and extra framework sites on the location of Al atoms in the low Si/Al regime.

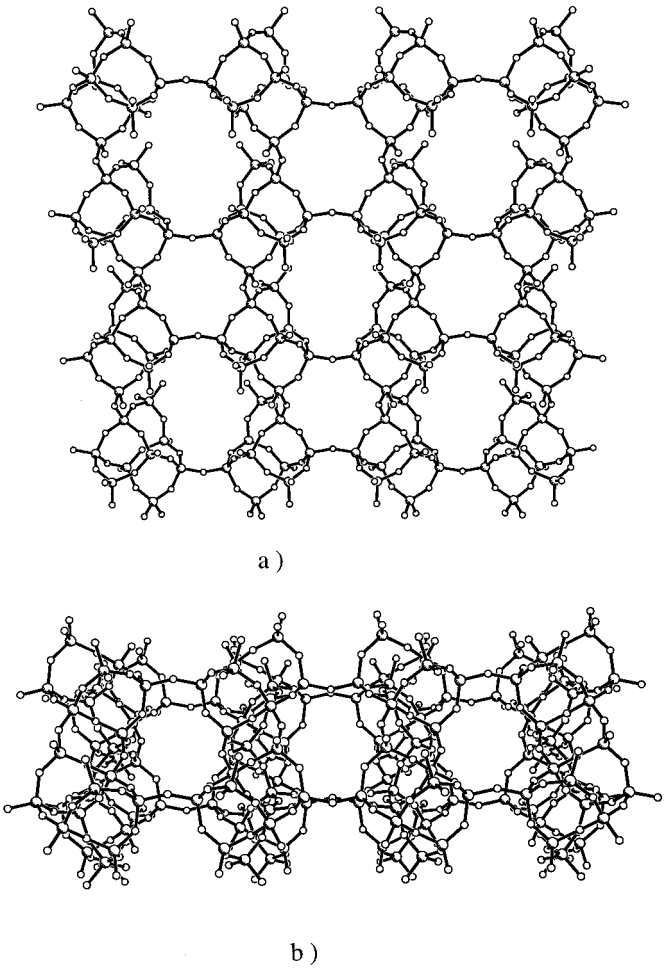

Figure 1. View of the topology of clinoptilolite: (a) along (001) showing channels in **a** and **b**, (b) along (100) showing channel in **c**, where **a**, **b**, and **c** are the relevant crystallographic directions.

2. Methodology

The calculations in this work were performed using lattice energy minimization techniques[16] employing the general utility lattice program (GULP) code.[36] The lattice energy calculation uses standard techniques based on the Ewald[37] method for summation of the long-range interactions and direct summation of the short-range interactions, which can be described by a number of potential forms. All atomic coordinates and cell parameters are optimized to zero force using the Broyden−Fletcher−Goldfarb−Shanno (BFGS) minimization method.[38] Any optimized structures, having imaginary phonon frequencies (i.e., a saddlepoint on the energy surface has been found rather than a minimum) were further optimized using the rational functional optimization (RFO) method,[39] to remove the imaginary modes. A convergence criteria of a gradient norm below 0.001 eV/Å was used for all of the calculations.

The interatomic potentials of Jackson and Catlow[40] were used, which use a Buckingham function to describe the short-range interactions, and a three-body (bond bending) term is included to model O−T−O angles accurately. A shell model[41] is used to simulate the polarizability of the oxygen atoms. The parameters used are given in Table 1. This model has proven successful in modeling the structure of many microporous materials[40,42−45] and has been used as an aid in determining the structure of such materials.[46,47]

TABLE 1: Interatomic Potential Parameters[a]

Buckingham potential	A (eV)	ρ (Å)	C (eV Å^6)
Si^{4+}—O^{2-}	1283.9	0.320 52	10.66
Al^{3+}—O^{2-}	1460.3	0.299 12	0.00
O^{2-}—O^{2-}	22 764.0	0.149 00	27.88
Na^{+}—O^{2-}	1226.8	0.306 50	0.00
three-body potential	k (eV rad^{-1})		θ_0 (deg)
O—T—O	2.097 24		109.47
core−shell potential	k (eV Å^{-2})		Y
O^{2-}	74.92		−2.869 02

[a] $V = \sum_{ij}$ (Buckingham) + $\sum_{ij}$(Coulomb) + $\sum_{ijk}$(three body) + $\sum_{ij}$(core−shell). V_{ij}(Buckingham) $= A_{ij} \exp(-r_{ij}/\rho) - C_{ij}/r^6$. V_{ij}(Coulomb) $= q_i q_j / r_{ij}$. V_{ijk}(three body) $= 0.5\, k_{ijk}\, (\theta_{ijk} + \theta^0_{ijk})^2$. V_i(core−shell) $= 0.5\, k_i\, \Delta r_i^2$, where Δr_i is core−shell separation. T is any tetrahedral atom (Al or Si). Y is the shell charge. All short-range interactions are cutoff for distances >12 Å.

Atomic coordinates for the tetrahedral and oxygen atoms positions were taken from the experimental structure determination of Alberti[48] for the minimization of a purely siliceous clinoptilolite unit cell. To construct a unit cell of an idealized Na—clinoptilolite (natural materials always contain a mixture of cations) with a Si/Al ratio of 5, the chemical formula is $Na_6Al_6Si_{30}O_{72}$, requiring 6 Al to be distributed over 36 T sites, for which there exist more than 1.9 million possible combinations, and among them around 200 000 satisfy Lowenstein's rule. The time required for the optimization of all configurations (even the 200 000 Lowensteinian configurations) is prohibitive. An alternative methodology is clearly required.

We base our approach on the fact that Al incorporation causes significant local distortions. If we consider the structure of clinoptilolite (Figure 1), we propose that structures that are least stressed and more stable should be those which satisfy the following two criteria: (1) They contain three Al atoms in each half of the unit cell. Alternative possibilities necessarily involve configurations of 4:2, 5:1, and 6:0 Al atoms in each half of the unit cell, which may result in significant unfavorable distortion of the structure. (2) Pairs of Al atoms in the unit cell must be related by centrosymmetry, because the framework has been determined to be centrosymmetric.[48] This constraint is only enforced for the initial construction of trial unit cells; all of the symmetry constrains are removed during energy minimization.

We determined that there are 324 different configurations that meet these criteria, of which 118 are non-Lowensteinian. However, here we will also consider these non-Lowensteinian configurations because we note that Bell et al. found that such configurations in zeolite A are in some cases only unfavorable by a small amount of energy.[24] The construction of trial unit cells in this manner can be applied generally to zeolitic structures, although at present different topologies and space-groups would require individual treatment.

To obtain reasonable initial atomic positions for the framework Al we used those obtained by calculating the geometry for the dilute case in which one Al—Na pair is introduced into a perfect lattice of siliceous clinoptilolite using the Mott—Littleton methodology.[17] The calculated coordinates of these distorted AlO_4 tetrahedra are used as starting geometries of the T sites in the full unit cell calculations.

The choice of the initial coordinates of the Na are not as straightforward because there are a number of potential sites and also other considerations. Although in the Mott—Littleton calculations we have determined the minimum energy sites for cations near each T site, we have not used these coordinates here, because in many cases (on construction of the periodic unit cell) close Al—Al distances will result in the (Mott—Littleton) calculated cation sites being too close to each other to be reasonable (<∼4 Å). We have therefore placed them each time at the same sites in the channels to prevent biasing the calculations and allowed the minimization procedure to optimize their position. We place one Na in each of the two 8-member cavities and two Na in each of the two 10-member cavities. The Na were located in the center of the 8-member cavities, whereas their location in the 10-member cavities was such that the Coulombic repulsions were minimized. Both of these positions will be much higher in energy than the final cation siting while at the same time, they are likely to lie on an energy gradient unlikely to be hindered in any way from reaching the minimum. Such optimizations may not be the case if the Mott—Littleton positions were used, because cations may have to move from one channel into another; a difficult task for an energy minimization routine.

TABLE 2: Lattice Parameters and Space Group (SG) for the Experimental Clinoptilolites[48] (a) Agoura Clinoptilolite, (b) Alpe Di Siusi Clinoptilolite, and Our Calculated Pure Si—Clinoptilolite

cell	a (Å)	b (Å)	c (Å)	β (°)	SG
experiment (a)	17.646	17.898	7.397	116.22	C2/*m*
experiment (b)	17.637	18.024	7.399	116.23	C2/*m*
calculated (for purely siliceous structure)	17.482	17.549	7.344	116.359	C2/*m**

*Space group determined using the program of Le Page.[53]

3. Results and Discussion

3.1. Al Incorporation as a Defect in Pure Si—Clinoptilolite. Table 2 shows the lattice parameters of the pure Si—clinoptilolite obtained in this work. This lattice will be the host for the Al—Na incorporation. The experimental lattice parameters obtained by Alberti[48] are also included in the same table. The differences are a consequence of treating the unit cell as siliceous (neglecting the Al and Na); we will show later how the already good agreement is further improved by the construction of more accurate unit cell models.

To illustrate the local distortions caused by the incorporation of Al as an isolated defect in the siliceous unit cell, we present the local geometry around the five unique T-sites of the pure Si—clinoptilolite and those after incorporation of an isolated Al substitutional. The T—O bond lengths are given in Tables 3 and 4 for the pure Si—clinoptilolite and isolated Al site in Si—clinoptilolite, respectively, in which the atoms are labeled as shown in Figure 2a. For an Al substitutional, the Si—O bond lengths in the Al—O—Si bridges are also shown.

In the pure Si—clinoptilolite, all Si—O distances are very close to an average value of 1.602 Å, which is in good agreement with typical experimental T—O distances found in aluminosilicates.[49] The substitution of silicon by aluminum results in longer Al—O bonds (on average 1.713 Å) and a shortening of the neighboring Si—O distances. The longest experimental T—O distances reported by Alberti[48] are 1.65 and 1.68 Å for Agoura and Alpe di Siusi clinoptilolites, respectively, and the shortest is 1.60 Å in both materials. The increase in the Al—O distance is well understood on an electrostatic basis, but this does not explain the reduction of the Si—O distances. We note that the simulations of Jackson and Catlow[40] also showed similar shortening of Si—O bond lengths in low Si/Al structures and this may be a consequence of the Si—O potential being too soft.

TABLE 3: Si−O (Å) Bond Lengths of the Calculated Pure Si−Clinoptilolite (Numbers in Brackets Refer to the Alberti Asymmetric Unit Cell)[48]

Si(1)		Si(2)		Si(3)		Si(4)		Si(5)	
O(3)	1.599	O(1)	1.589	O(2)	1.591	O(5)	1.599	O(6)	1.606
O(4)	1.603	O(2)	1.602	O(3)	1.600	O(7)	1.606	O(6)	1.606
O(6)	1.602	O(4)	1.613	O(7)	1.599	O(8)	1.594	O(8)	1.597
O(9)	1.615	O(10)	1.599	O(9)	1.609	O(10)	1.598	O(8)	1.597

TABLE 4: Al−O (Å) Distances When Al Atoms Are Treated as Defects in a Pure Si−Clinoptilolite; Si−O (Å) Distances and Si Atoms Are Those That Belong to the Al−O−Si Bridges (Numbers in Brackets Refer to the Alberti Asymmetric Unit Cell)[48]

Al (1)		Al (2)		Al (3)		Al (4)		Al (5)	
O(3)	1.689	O(1)	1.683	O(2)	1.722	O(5)	1.736	O(6)	1.757
O(4)	1.743	O(2)	1.703	O(3)	1.738	O(7)	1.689	O(6)	1.757
O(6)	1.738	O(4)	1.764	O(7)	1.691	O(8)	1.686	O(8)	1.681
O(9)	1.703	O(10)	1.677	O(9)	1.701	O(10)	1.730	O(8)	1.681
Si		**Si**		**Si**		**Si**		**Si**	
O(3)	1.550	O(1)	1.525	O(2)	1.565	O(5)	1.567	O(6)	1.577
O(4)	1.578	O(2)	1.544	O(3)	1.569	O(6)	1.549	O(6)	1.577
O(6)	1.572	O(4)	1.569	O(7)	1.558	O(8)	1.548	O(8)	1.542
O(9)	1.567	O(10)	1.540	O(9)	1.565	O(10)	1.566	O(8)	1.542

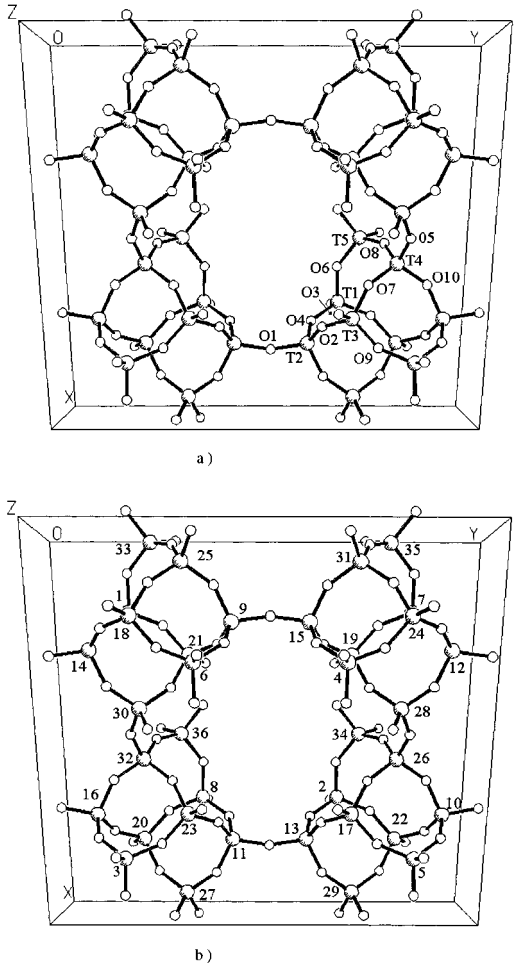

Figure 2. Unit cell of the clinoptilolite: (a) asymmetric unit cell of Alberti,[48] (b) identification of the T atoms in the unit cell as used in this work. Small spheres are oxygen, and larger spheres are tetrahedral silicon or aluminum.

The T−O−T angles are also an important geometric parameter in the structure of zeolites. The Si−O−Si angles of the pure Si−clinoptilolite are presented in Table 5 and those for the defect Al containing clinoptilolite are presented in Table 6. Comparing the values from these tables, we can see that the T−O−T angles are strongly modified by the presence of Al; at least one of the Al−O−Si angles has decreased by about 10°. Note that some angles are very low (around 130°), which is lower than those typically encountered in Si−O−Si bridges.[49] This kind of distortion also introduces stress in the lattice, and has been identified as one of the factors which causes instability in zeolite frameworks.[44,50]

The substitution energies for the incorporation of the Al−Na pairs in the pure Si−clinoptilolite structure are presented in Table 7. The lowest energy is found for the T3 site, and the highest energy is encountered for the T2 site; a result also noted by Channon et al.[34] Experimentally, a higher occupancy of Al atoms was found at T2 sites, so these two results are contradictory. We will address this problem in the next section.

Note that the lowest substitution energies—at sites T3 and T4−(Tables 5 and 6) are found for sites which have four Si−O−Si angles around 150° in the perfect lattice. Even after incorporation of the Al in these sites, the lowest T−O−T angles (∼140°) remain in the range typically found in zeolites. We also note that sites T1 and T5 exhibit lower T−O−T angles and have similar substitution energies, suggesting a relationship between the bond angle and the defect energy. However, for the T2 site, this does not appear to be the case: the higher substitution energy does not appear to be a consequence of low T−O−T angles. Thus, it is clear that the problem of the siting of Al atoms is not a simple one, and it appears that longer-range interactions (i.e., the Madelung potential) may be dominant.

3.2. Al Distribution in the Clinoptilolite Cell and the Obeyance of Lowenstein's and Dempsey's Rules. We now consider the energetics and geometries of the 324 optimized unit cells constructed according to the discussions above. Table 8 shows the 10 configurations with the lowest lattice energies of all the configurations considered, with both initial and final lattice energies presented. The numbers in the second column indicate the aluminum atoms of each distribution; the positions of the T sites labeled by these numbers are shown in Figure 2b.

We note that, in these most stable configurations (Table 8), aluminum atoms are located preferentially at T2 sites (indicated in bold), whereas no Al atoms are found at T5 sites. This result agrees with the higher occupancy of T2 found experimentally by Alberti.[48] Although the absence of Al atoms in sites T5

TABLE 5: Si−O−Si Angles (deg) of the Optimized Pure Silica Clinoptilolite

Si(1)−O−Si		Si(2)−O−Si		Si(3)−O−Si		Si(4)−O−Si		Si(5)−O−Si	
O(3)−Si(3)	149.79	O(1)−Si(2)	154.75	O(2)−Si(2)	151.58	O(5)−Si(4)	146.94	O(6)−Si(1)	141.18
O(4)−Si(2)	139.12	O(2)−Si(3)	151.58	O(3)−Si(1)	149.79	O(7)−Si(3)	154.27	O(6)−Si(1)	141.18
O(6)−Si(5)	141.18	O(4)−Si(1)	139.12	O(7)−Si(4)	154.27	O(8)−Si(5)	151.32	O(8)−Si(4)	151.31
O(9)−Si(3)	149.07	O(10)−Si(4)	150.13	O(9)−Si(1)	149.07	O(10)−Si(2)	150.13	O(8)−Si(4)	151.31

TABLE 6: Al−O−Si Angles (deg) of the Optimized Isolated Al Site in an Otherwise Siliceous Clinoptilolite

Al(1)−O−Si		Al(2)−O−Si		Al(3)−O−Si		Al(4)−O−Si		Al(5)−O−Si	
O(3)−Si(3)	148.03	O(1)−Si(2)	154.90	O(2)−Si(2)	142.34	O(5)−Si(4)	137.69	O(6)−Si(1)	131.80
O(4)−Si(2)	129.88	O(2)−Si(3)	146.68	O(3)−Si(1)	138.62	O(7)−Si(3)	154.62	O(6)−Si(1)	131.79
O(6)−Si(5)	134.03	O(4)−Si(1)	129.74	O(7)−Si(4)	150.63	O(8)−Si(5)	149.06	O(8)−Si(4)	152.82
O(9)−Si(3)	145.53	O(10)−Si(4)	154.99	O(9)−Si(1)	148.12	O(10)−Si(2)	141.34	O(8)−Si(4)	152.78

TABLE 7: Calculated Defect Energies (eV); (Numbers in Brackets Refer to the Alberti Asymmetric Unit Cell)[48]

T	defect energy (eV)
Al(1)	33.27
Al(2)	33.32
Al(3)	33.03
Al(4)	33.18
Al(5)	33.24

TABLE 8: The 10 Al Atoms Configurations Having Lowest Lattice Energies; See Text for Details (T Sites Are T1, 1−8; T2, 9-16; T3, 17-24; T4, 25-32; T5, 33-36)

order	position of Al atoms	initial lattice energy (eV)	final lattice energy (eV)
1	**11**, **12**, **15**, **16**, 17, 21	−4400.7	−4431.3
2	2, 6, **11**, **12**, **15**, **16**	−4402.1	−4431.0
3	1, 5, 19, 23, 27, 31	−4395.9	−4430.9
4	**11**, **12**, **15**, **16**,18, 22	−4400.7	−4430.8
5	1, 5, **11**, **12**, **15**, **16**	−4402.1	−4430.7
6	**9**, **12**, **13**, **16**, 19, 23	−4399.3	−4430.7
7	4, 8, **12**, **16**, 17, 21	−4399.8	−4430.7
8	**12**, **16**, 18, 19, 22, 23	−4396.9	−4430.7
9	4, 8, **12**, **16**, 18, 22	−4399.5	−4430.7
10	17, 19, 20, 21, 23, 24	−4395.0	−4430.7

was not revealed by the study of Alberti,[48] Koyama and Takeuchi[51] report that T5 has the lowest Al occupancy for one of their samples.

The isolated substitution energies for the various T sites (see Table 7) do not provide an obvious explanation for Al distribution suggested by the results in Table 8. However, interactions between framework Al will be strong in such a high Al content material, and such interactions change the relative energies of the different T-site occupancies. Channon et al. also report such a modification.[34] Clearly, care should be taken when extrapolating information gained from such calculations on isolated configurations of any preferential siting when higher Al concentrations are considered. This factor will be particularly important when aluminum levels such as those encountered in clinoptilolite are considered.

Figure 3 shows a plot of the initial and final lattice energy of the 324 structures considered. Although many of those configurations with a high initial lattice energy remain higher in energy after lattice relaxation, there are several other cases for which this does not apply. It is clear, therefore, that it is not possible to identify favorable configurations from the sample by performing a single point energy calculation. We conclude, therefore, that Monte Carlo sampling based on single point calculations may not identify the lowest energy configurations and in such systems, lattice relaxation is clearly required.

The lattice energies (initial and final) of the 10 least stable Lowensteinian configurations are presented in Table 9 in which we note the presence of Al atoms at T5 sites (indicated in bold)

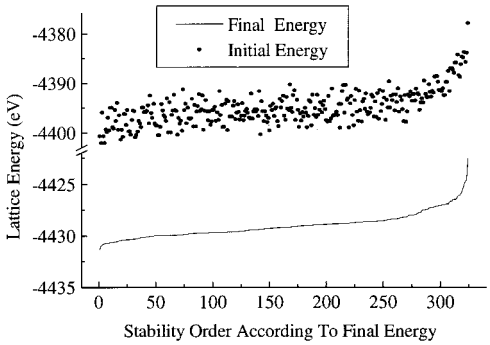

Figure 3. Initial and final energies of the 324 configurations versus the stability order according to the final energy.

TABLE 9: The 10 Al Atoms Configurations Having Highest Lattice Energies; See Text for Details (T Sites Are T1, 1−8; T2, 9−16; T3, 17−24; T4, 25−32; T5, 33-36)

order	position of Al atoms	initial lattice energy (eV)	final lattice energy (eV)
1	12, 16, 26, 30, **33**, 35	−4384.2	−4427.7
2	4, 8, 17, 21, **33**, **35**	−4388.3	−4428.7
3	19, 20, 23, 24, **34**, **36**	−4388.7	−4428.9
4	4, 8, 9, 13, **33**, **35**	−4386.2	−4428.9
5	2, 6, 11, 15, **33**, **35**	−4384.7	−4428.9
6	4, 8, 9, 13, 27, 31	−4384.8	−4428.9
7	12, 16, 19, 23, **34**, **36**	−4383.7	−4429.0
8	12, 16, 26, 27, 30, 31	−4385.7	−4429.0
9	10, 14, 28, 32, **33**, **35**	−4383.8	−4429.1
10	9, 13, 19, 23, 27, 31	−4377.8	−4429.1

in the five configurations with highest energies. The high energy of such configurations appears to be due to a combination of electrostatic and geometric factors because T5 atoms are located within the wall of the channel (rather than at the edge of the channel wall for T1−3). Consequently, the distance between these $Al(5)O_4$ tetrahedra and both experimental Na sites and also any other possible extraframework site are significantly longer than possible for the other T sites. Interestingly, we find that in each one of these 10 configurations there exists at least one Na atom which is not coordinated to any tetrahedron containing Al atoms. These results reinforce the relationship between Al atoms and extraframework cations.[29] We will discuss in detail the structure of the most stable unit cell later.

The lowest energy non-Lowensteinian configuration is less stable than the most stable configuration by 1.40 eV (Table 8). In this non-Lowensteinian configuration, all of the Al atoms are located at T2 sites and form two Al−O−Al bridges. This is in accordance with the results of Slaughter et al.,[32] who suggested that breaking of Lowenstein's rule could occur in heulandites but only at T2 sites. The lowest energy non-Lowensteinian configuration which has no Al atoms at T2 is 0.43 eV less stable than the above configuration. However,

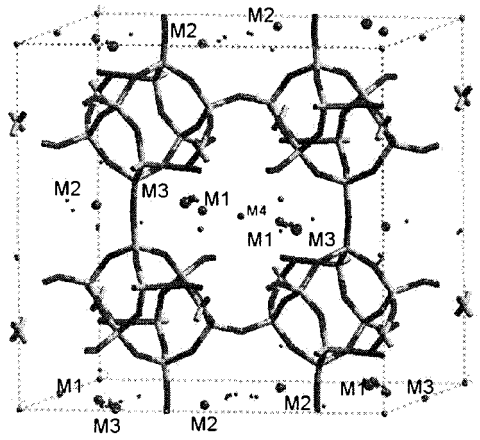

Figure 4. Distribution of extraframework Na cations in the 10 most stable calculated configurations. The larger spheres are the experimental sites of Alberti[48] labeled C1, C2, and C3 and those of Koyama and Takeuchi[51] labeled M1, M2, M3, and M4; C1 is equivalent to M1 and C2 is equivalent to M2. The smaller spheres are the cation positions calculated in the 10 most stable configurations. Note that many of these overlap and are also located at exactly the experimental site.

we should also note that several configurations satisfy the Lowenstein rule which have higher lattice energies than a number of non-Lowensteinian configurations; thus the framework topology has special significance in determining the Al location. As noted earlier, Catlow et al.[27] suggested that Lowenstein's rule is a consequence of the energetics of the reaction of small gel species; formation of Al−O−Al bonds is much less energetically favorable than formation of Al−O−Si bonds. However, it is probable that the presence of other cations at this precursor stage could provide additional thermodynamic stability which may result in Lowenstein's rule, and certainly Dempsey's rule, being broken.

Considering Dempsey's rule in greater details, the Al-*n*(O−Si−O)-Al linkages presented in our models have *n* values between 0 and 2. Although the two most stable structures have maximum Al−Al distances ($n = 2$), structures such as the third and sixth to ninth of Table 8 contain Al−O−Si−O−Al bridges. It is, however, evident that the most stable configurations do indeed obey both Lowenstein's and Dempsey's rule. However, as suggested above, there may be a degree of "shielding" because of the presence of the extraframework sodium cations which would stabilize closer Al−Al distances than those expected if Dempsey's rule is strictly obeyed.

3.3. Location of the Extraframework Cations: Comparison to Diffraction Data. Although we have concentrated here on the distribution of the framework Al, we have also analyzed the siting of the extraframework cations in our calculated structures. From an analysis of the 10 most favored configurations it is clear that our simulation technique is correctly locating the cations, not only at geometrically reasonable sites, but also at (or close) to experimentally determined positions. In the following discussion the cation sites are labeled as denoted by Alberti[48] (C1, C2, C3) and by Koyama and Takeuchi[51] (M1...M4). Figure 4 shows the distribution of Na cations in the most favored configurations, and Table 10 gives average cation−framework distances for the 10 most- and least-favored configurations. The distribution of cations can be summarized as follows:

(1) The site denoted C1[48] (equivalent to M1[51]) is almost fully occupied in the 10 most stable configurations—8 of the 10 configurations are fully occupied—which is in excellent agreement with experimental data on natural samples which show not only full occupancy of this site but also almost exclusive occupancy by sodium cations. However, the calculated positions (Table 10) are much closer to the framework than in the experimental structures (∼2.83 Å[51]). Indeed, the cations are more correctly described as midway between the M1 (C1) site and the M3 site.[51] We note that experimentally, the M3 site is occupied by K^+ and is the least hydrated cation site.[51] We therefore propose that the differences between our calculated sites and those found by diffraction are because our simulations, unlike the experiments, relate to the dehydrated system. Indeed we would expect the presence of water to increase the coordination number of the extraframework cations and to weaken the interaction of those cations with the framework, thus allowing longer cation-framework distances. Conversely, where no water is present, an increase in the coordination to the framework would be expected, which is reflected in the average coordination number and closer cation−framework distances in our simulations.

TABLE 10: Average Geometric Parameters for the Extraframework Na Cations; Averages Are Calculated for the 10 Most and Least Stable Configurations

	low energy (Å)	high energy (Å)
Na coordination number	4.03	3.93
Na−O distance	2.51	2.50
Na−Al distance	3.63	4.39

(2) Site C2[48] (equivalent to M2[51]) is approximately 50% occupied over the 10 configurations, although again the calculated position is closer to the framework oxygens. We also note that in cases of lower occupation of C1, we find increased C2 site occupancy. Experimentally,[48,51] the C2 site is more favorably occupied by Ca^{2+} than by Na^+ and this is reflected in these results by the domination of C1 site occupancy in our ideal sodium-only form.

(3) Only one of the 10 most stable configurations has a cation at the site denoted C3 and no cations are found at the site denoted M4; we note that these two sites have low occupation in the natural samples and are occupied solely by larger cations such as potassium and calcium.[51] However, we also note that the C3 site is occupied in a small number of the less favored configurations.

(4) The average coordination number and the nearest oxygen distance remains reasonably constant regardless of the energy of the configuration (Table 10). However, we see an increase in the average Na−Al distance from the low energy to the high energy configurations, suggesting that the stability of a particular configuration is heavily influenced by the manner in which the cations can coordinate to the framework. In particular we note that some of the high-energy configurations have Al located in such a way as to prevent the cations being located at the optimal position due to close Al−Al distances (see the discussion above regarding T5 occupation and similar discussion by Channon et al.[34]), which results in increased Al−Na distances as reflected in the increase average Al−Na distance in the less favorable configurations.

The cation sites identified by our calculations appear to be consistent with those identified by experiment. However, it would be interesting to determine experimentally the cation sites in dehydrated samples. Furthermore, the natural samples always contain a mixture of cations. The recent developments in the preparation of synthetic heulandites and clinoptilolites, in which where cation composition can be controlled,[52] will allow more detailed comparison between the predictions of our calculations and experiment.

TABLE 11: Coordinates for the Most Stable Na Clinoptilolite Unit Cell Configurations (*P*1) (Cell Parameters Are $a = 17.619$ Å, $b = 17.805$ Å, $c = 7.374$ Å, $\alpha = 88.311°$, $\beta = 116.213°$, and $\gamma = 91.565°$)

	x	*y*	*z*		*x*	*y*	*z*		*x*	*y*	*z*
Si	0.1806	0.1782	0.7480	Na	0.5278	0.0002	0.0972	O	0.9239	0.1751	0.5999
Si	0.6735	0.6738	0.7583	Na	0.0333	0.4963	0.1023	O	0.4180	0.6811	0.6100
Si	0.8263	0.1745	0.5610	Na	0.2135	0.9993	0.4813	O	0.9251	0.8391	0.6230
Si	0.3208	0.6769	0.5705	Na	0.7895	0.0126	0.7967	O	0.4296	0.3339	0.5917
Si	0.8248	0.8337	0.5587	O	0.1931	0.5030	0.1245	O	0.0817	0.8374	0.7071
Si	0.3322	0.3381	0.5490	O	0.7043	0.0009	0.1105	O	0.5877	0.3329	0.6940
Si	0.1789	0.8387	0.7425	O	0.8068	0.5087	0.1898	O	0.1292	0.2318	0.2056
Si	0.6851	0.3371	0.7325	O	0.2938	0.0112	0.2005	O	0.6198	0.7342	0.1920
Si	0.2227	0.4194	0.1441	O	0.7362	0.6128	0.3004	O	0.8870	0.2366	0.1093
Si	0.7196	0.9153	0.1580	O	0.2393	0.1269	0.2836	O	0.3785	0.7429	0.1110
Al	0.7900	0.4176	0.1233	O	0.2660	0.6339	0.0491	O	0.8756	0.7823	0.1013
Al	0.2841	0.9192	0.1350	O	0.7703	0.1304	0.0335	O	0.3830	0.2789	0.1138
Si	0.7813	0.5929	0.1637	O	0.2651	0.4005	0.0015	O	0.1186	0.7720	0.1958
Si	0.2851	0.0968	0.1495	O	0.7628	0.8864	0.0182	O	0.6277	0.2657	0.1972
Al	0.2149	0.5958	0.1800	O	0.7358	0.3767	0.2445	O	0.0227	0.2779	0.8399
Al	0.7196	0.0938	0.1682	O	0.2303	0.8816	0.2624	O	0.5129	0.7910	0.8351
Al	0.7051	0.6915	0.3797	O	0.6812	0.6500	0.5633	O	0.9925	0.2862	0.4654
Si	0.2138	0.1962	0.3777	O	0.1939	0.1540	0.5498	O	0.4898	0.7868	0.4683
Si	0.2954	0.7004	0.9512	O	0.3184	0.6607	0.7858	O	0.9844	0.7358	0.4613
Si	0.8019	0.1983	0.9433	O	0.8241	0.1580	0.7770	O	0.4938	0.2236	0.4654
Al	0.2982	0.3214	0.9248	O	0.3231	0.3630	0.7418	O	0.0142	0.7239	0.8354
Si	0.7909	0.8166	0.9282	O	0.8108	0.8590	0.7555	O	0.5184	0.2244	0.8330
Si	0.7094	0.3117	0.3508	O	0.6867	0.3519	0.5157	O	0.2153	0.2586	0.8240
Si	0.2018	0.8137	0.3583	O	0.1795	0.8537	0.5243	O	0.7153	0.7570	0.8370
Si	0.0761	0.3013	0.0693	O	0.7200	0.6104	0.9256	O	0.7874	0.2548	0.4641
Si	0.5687	0.8039	0.0740	O	0.2266	0.1114	0.9099	O	0.2776	0.7551	0.4646
Si	0.9411	0.3091	0.2290	O	0.2741	0.6063	0.4400	O	0.7879	0.7544	0.4799
Si	0.4357	0.8131	0.2361	O	0.7768	0.1058	0.4267	O	0.2897	0.2557	0.4689
Si	0.9277	0.7107	0.2339	O	0.2858	0.4016	0.3796	O	0.2190	0.7586	0.4689
Si	0.9277	0.7107	0.2339	O	0.2858	0.4016	0.3796	O	0.2190	0.7586	0.8406
Si	0.4345	0.2084	0.2288	O	0.7799	0.9012	0.3963	O	0.7284	0.2587	0.8386
Si	0.0619	0.7017	0.725	O	0.7318	0.4078	0.8611	O	0.1326	0.3741	0.0825
Si	0.5676	0.1987	0.0664	O	0.2282	0.9076	0.8752	O	0.6265	0.8796	0.0952
Si	0.0047	0.2283	0.6458	O	0.0119	0.3322	0.1497	O	0.8896	0.3821	0.1965
Si	0.4990	0.7345	0.6566	O	0.5043	0.8380	0.1527	O	0.3848	0.8861	0.2165
Si	0.0012	0.7834	0.6573	O	0.9889	0.6808	0.1434	O	0.8685	0.6420	0.2281
Si	0.5075	0.2785	0.6463	O	0.4956	0.1759	0.1384	O	0.3767	0.1347	0.2176
Na	0.2949	0.5058	0.7726	O	0.0802	0.1716	0.6843	O	0.1124	0.6267	0.1060
Na	0.7117	0.5074	0.5249	O	0.5762	0.6781	0.7177	O	0.6162	0.1227	0.0896

3.4. Relative Stability of the Lowest Energy Configuration Compared to Those of Alternate Models. To verify the assumptions described in the methodology section regarding the configurations evaluated, we constructed a number of unit cells which were either noncentrosymmetric or did not contain three Al in each half of the cell. Taking our lowest energy configuration as a starting point, we made modifications to the siting of the Al atoms so that the T2 sites were preferentially occupied (as suggested by our results). Thus, we maintained Al occupancy of the four Al atoms in positions 11, 12, 15, and 16 (Figure 2b and Table 8) and the other remaining two Al atoms were located in all possible combinations. Each new unit cell was then submitted to the same energy minimization procedure as applied above, i.e., all atomic coordinates and cell parameters were optimized to zero force.

When we located four and two Al atoms in the upper and lower halves of the unit cell, respectively, we found that these configurations were highly unfavorable. The lowest energy configuration in this case has a lattice energy which is higher by 1.2 eV than that of configuration 1 of Table 8.

When a distribution of three Al atoms in each half of the unit cell was maintained, but noncentrosymmetry between Al atoms pairs was permitted, higher lattice energies also resulted. However, when cells with Al atoms in positions 2, 11, 12, 15, 16, 21 and in positions 6, 11, 12, 15, 16, 17, the lattice energies are −4431.14 eV, which are only 0.20 eV less favorable than the lowest energy found in our model. These two configurations are closely related to the most stable unit cell, the differences being the exchange of an Al atom from site 17 to 2 in the first and from 21 to 6 in the latter (Figure 2b). It is clear that the local environments of these sites are very similar, having similar coordinates in the *ab* plane, whereas the major difference is in *z* coordinate. Similarly this modification in framework configuration requires little change in the extraframework cation positions. Our results therefore suggest that symmetry constrains are less important (as we may expect) than that of Al partitioning in searching for the absolute lowest energy configuration; that is, changing (indeed, reduction) the symmetry is less likely to introduce strain, whereas partitioning of the Al in the unit cell leads to more strained Al−Al interactions.

3.5. The Calculated Lowest Energy Unit Cell. The calculated lattice parameters are 17.619, 17.805, and 7.374 Å, which are in excellent agreement with experimental determinations (for example, the values reported in refs 48 and 51 are in the range $a = 17.646-17.662$ Å, $b = 17.898-17.963$ Å, and $c = 7.397-7.407$ Å) and are an improvement on the agreement found for the siliceous unit cell considered previously. The cell angles, 88.311°, 116.213°, and 91.565°, are also in good agreement with experimental values (β is typically 116.36−116.47° [48,51]). The atomic coordinates of this lowest energy unit cell are presented in Table 10. The remaining discrepancies are likely to be a consequence of differences in composition; for example, the natural samples have Si/Al ∼4.7 and will also contain other cations. However, the dehydrated nature of our simulations is the likely source of the differences in the location of extraframework cation sites. We also stress that our

calculations are effectively at 0 K, whereas experimental structural determinations were performed at room temperature.

Symmetry analysis[53] was performed for three cases: the full unit cell, the full unit cell without distinction between Si and Al atoms, and only the framework atoms, again without differentiation between Si and Al. In all three cases no symmetry elements (*P*1 space group) were found. We note that no thermal motion is included in our model and this may account for the low symmetry. It is also obvious that a material will consist of many of our configurations and not a single cation and aluminum distribution.

Given the low symmetry of the cell we do not present the explicit T−O distances and T−O-T angles; they are not the main goal of our analysis. However, we note the following: (1) In the Al−O−Si bridges the Al−O and Si−O bond lengths are on average 1.71 and 1.56 Å, respectively, and are similar to the results obtained for the isolated Al defect (section 3.1). (2) The average T−O bond distance (where Al and Si are equivalent) is 1.624 Å, which is in excellent agreement with the values of 1.621 Å[48] and 1.625 Å[51] found experimentally. (3) The values of T−O−T angles show a wide range from 140 to 160°, a result that indicates that the primary mode of relaxation of the cell is by changes in the T−O−T angles rather than in T−O distances.

4. Conclusions

We have presented a novel procedure, which has been successfully used in a computer simulation study of the hitherto unsolved problem of Al siting in zeolites. The results suggest that in order to find the absolute energy minima it is necessary, in addition to determining the model configurations that obey symmetry and accepted Al distribution rules, to scan those configurations which are close to the lowest energy distributions but which break the imposed symmetry constraints. Furthermore, it is clear how lattice relaxation is of the utmost importance in determining the atomic distribution. Thus, a Monte Carlo approach based on unrelaxed lattice energies is not suitable for identifying potential configuration of cations and Al distributions in such materials.

In summary, our main results regarding the structure and Si−Al distribution in clinoptilolite are (i) high preference for T2 sites and very low occupancy of T5 sites, and (ii) the lowest energy configuration possesses Al distributions which obey both Lowenstein's and Dempsey's rules.

We would consider it valuable to reevaluate the crystallographic refinements in the light of our calculations regarding relative occupation of the T sites by Al and to determine experimentally the effect of dehydration on cation siting. Furthermore, given that preparation of samples, with control over the extraframework cation composition is now possible,[52] it would be interesting to determine the cation location in such samples compared to our calculations.

From a methodological point of view we remark that energies of isolated Al substitutions (either from Mott−Littleton or quantum mechanical cluster calculations) may give different results regarding preferential Al occupancy than those obtained using periodic unit cells when *high* Al content zeolites are considered. Clearly, interactions between close-neighbor Al atoms and compensating cations have a critical influence on the atomic distributions.

The application of our procedure to the study of heulandite, the natural Ca-bearing analogue of clinoptilolite, and mixed cation clinoptilolites, will be the topic of future investigations.

Acknowledgment. We thank Ariel Gómez for his assistance in the determination of the symmetry of the unit cells and for his stimulating comments. We also thank Prof. Luis Montero for many helpful discussions.

References and Notes

(1) Ramdas, S.; Thomas, J. M.; Fyfe, C. A.; Hartman, J. S. *Nature* **1981**, *292*, 228.
(2) Engelhart, G.; Lohse, U.; Lippman, E. M.; Tarsmak, M.; Magi, M. Z. *Anorg. Allog. Chem.* **1982**, *482*, 49.
(3) Nagy, J. B.; Bodart, P.; Collette, H.; El Hage-Al Assward, J.; Gabelica, Z.; Aiello, R.; Nastro, A.; Pellegrino, C. *Zeolites* **1988**, *8*, 209.
(4) Takaishi, T.; Kato, M.; Itabashi, K. *Zeolites* **1995**, *15*, 21.
(5) Schroder, K.-P.; Sauer, J. *J. Phys. Chem.* **1994**, *98*, 5742.
(6) Derouane, E. G.; Fripiat, J. G. *Zeolites* **1995**, *15*, 21.
(7) Herrero, C. P. *J. Phys. Chem.* **1991**, *95*, 3282.
(8) Schroder, K.-P.; Sauer, J.; Leslie, M.; Catlow, C. R. A.; Thomas, J. M. *Chem. Phys. Lett.* **1992**, *188*, 320.
(9) Engelhardt, G.; Michel, D. *High-Resolution Solid State NMR of Silicates and Zeolites*; Wiley: New York, 1987.
(10) Klinowski, J. *Prog. NMR Spectrosc.* **1984**, *16*, 237.
(11) Pisani, C.; Dovesi, R.; Roetti, C. *Hartree−Fock Ab-initio Treatment of Crystalline Systems*; Springer-Verlag: Berlin, 1988; Lecture Notes in Chemistry, Vol. 48.
(12) Shah, R.; Payne, M. C.; Lee, M. H.; Gale, J. D. *Science* **1996**, *271*, 1395.
(13) Olson, D. H.; Kokotailo, G. T.; Lawton, S. L.; Meier, W. M. *J. Phys. Chem.* **1981**, *85*, 2238.
(14) van Koningsveld, H.; Jansen, J. C.; van Bekkum, H. *Zeolites* **1990**, *10*, 235.
(15) Schroder, K.-P.; Sauer, J.; Leslie, M.; Catlow, C. R. A. *Zeolites* **1992**, *12*, 20.
(16) *Computer Simulation of Solids*; Catlow, C. R. A.; Mackrodt, W. C., Eds.; Spinger-Verlag: Berlin, 1982; Lecture Notes in Physics, Vol. 166.
(17) Mott, N. F.; Littleton, M. J. *Trans. Faraday Soc.* **1938**, *34*, 485.
(18) Lewis, D. W.; Catlow, C. R. A.; Sankar, G.; Carr, S. W. *J. Phys. Chem.* **1995**, *99*, 2377.
(19) Jentys, A.; Catlow, C. R. A. *Catal. Lett.* **1993**, *22*, 251.
(20) Sastre, G.; Lewis, D. W.; Catlow, C. R. A. *J. Phys. Chem.* **1996**, *100*, 6722.
(21) Lowenstein, W. *Am. Miner.* **1854**, *39*, 92.
(22) Dempsey, E.; Kuhl, G. H.; Olson, D. H. *J. Phys. Chem.* **1969**, *73*, 387.
(23) Tarling, S. E.; Barnes, P.; Klinowski, J. *Acta Crystallogr.* **1988**, *B44*, 128.
(24) Bell, R. G.; Jackson, R. A.; Catlow, C. R. A. *Zeolites* **1992**, *12*, 870.
(25) Morales, J.; Bonilla-Marin, M.; Langagne, A. *Int. J. Quantum Chem.* **1991**, *25*, 659.
(26) den Ounden, C. J. J.; Jackson, R. A.; Catlow, C. R. A.; Post, M. F. M. *J. Phys. Chem.* **1990**, *94*, 5286.
(27) Catlow, C. R. A.; George, A. R.; Freeman, C. M. *J. Chem. Soc, Chem. Commun.* **1996**, 1311.
(28) Gramlich, V.; Meier, W. M. *Z. Kristallogr.* **1971**, *133*, 134.
(29) Breck, D. W. *Zeolite Molecular Sieves*; Wiley: New York, 1974; Chapter 7.
(30) Ames, L. L. *Am. Miner.* **1960**, *45*, 689.
(31) King, L. J.; Campbell, D. O.; Collins, E. D.; Knauer, J. B.; Wallace, R. M. In *Proceedings of the 6th International Conference on Zeolites*, Butterworths: Guildford, 1984; pp 660.
(32) Slaughter, M.; Yu, J.-Y. In *Natural Zeolites* '93. Int. Comm. Natural Zeolites; Ming, D. W., Mumpton, F. A., Eds.; Brockport, New York, 1993; p 209.
(33) (a) Channon, Y. M.; Catlow, C. R. A.; Jackson, R. A.; Owens, S. L. In *Zeolites: A Refined Tool for Designing Catalytic Active Sites*; Bonneviot, L., Kaliaguine, S., Eds.; Elsevier Science: Amsterdam, 1995; p 117. (b) Channon, Y. M.; Catlow, C. R. A.; Gorman, A. M.; Jackson, R. A.; *J. Phys. Chem. B*, **1998**, *102*, 4045.
(34) Channon, Y. M.; Catlow, C. R. A.; Jackson, R. A.; Owens, S. L. *Microp. Mesop. Mater.*, in press.
(35) Rodriguez-Fuentes, G.; Ruiz-Salvador, A. R.; Mir, M.; Picazo, O.; Quintana, G.; Delgado, M. *Microp. Mesop. Mater.* **1998,** *20*, 269.
(36) Gale, J. D. *J. Chem. Soc., Faraday Trans.* **1997**, *93*, 629.
(37) Ewald, R. P. *Ann. Physik* **1921**, *64*, 253.
(38) Shanno, D. F. *Math. Comput.* **1970**, *24*, 647.
(39) Simons, J.; Joergensen, P.; Taylor, H.; Ozment, J. *J. Phys. Chem.* **1983**, *87*, 2745.
(40) Jackson, R. A.; Catlow, C. R. A. *Mol. Simul.* **1988**, *1*, 207.
(41) Dick, B. G.; Overhauser, A. W. *Phys. Rev.* **1958**, *112*, 90.

(42) Bell, R. G.; Jackson, R. A.; Catlow, C. R. A. *J. Chem. Soc. Chem. Commun.* **1990**, 782.
(43) Henson, N. J.; Cheetham, A. K.; Gale, J. D. *Chem. Mater.* **1996**, *8*, 664.
(44) de Boer, K.; Jansen, A. P. J.; van Santen, R. A. *Phys. Rev. B* **1995**, *52*, 12579.
(45) Ruis-Salvador, A. R.; Sastre, G.; Lewis, D. W.; Catlow, C. R. A. *J. Mater. Chem.* **1996**, *6*, 1837−1842.
(46) Wright, P. A.; Natarajan, S.; Thomas, J. M.; Bell, R. G.; Gai-Boyes, P. L.; Jones, R. H.; Chen, J. *Angew. Chemie Int. Ed. Engl.* **1992**, *31*, 1472.
(47) Morris, R. E.; Weigel, S. J.; Henson, N. J.; Bull, L. M.; Janicke, M. T.; Chmelka, B. F.; Cheetham, A. K. *J. Am. Chem. Soc.* **1994**, *116*, 11849.
(48) Alberti, A. *Tschermaks. Mineral. Petrogr. Mitt.* **1975**, *22*, 25.
(49) Hill, R. J.; Gibbs, G. V., *Acta Crystallogr. B.* **1979**, *B35*, 25.
(50) Petrovic, Y.; Navrotsky, A.; Davies, M. E.; Zones, S. I. *Chem. Mater.* **1993**, *5*, 1805.
(51) Koyama, K.; Takeuchi, Y. *Z. Kristallogr.* **1977**, *145*, 216.
(52) Zhao, D.; Kevan, L.; Szostak, R. *Zeolites* **1997**, *19*, 366.
(53) Le Page, Y. *J. Appl. Crystallogr.* **1988**, *21*, 983.